Significant Performance Improvement of Porphyrin-Sensitized TiO2 Solar Cells under White Light Illumination

ARTICLE *in* THE JOURNAL OF PHYSICAL CHEMISTRY C · DECEMBER 2010

Impact Factor: 4.77 · DOI: 10.1021/jp107615h

8 AUTHORS, INCLUDING:

Matt Griffith
University of Newcastle
26 PUBLICATIONS **383** CITATIONS
SEE PROFILE

Michael James
Australian Synchrotron
148 PUBLICATIONS **2,242** CITATIONS
SEE PROFILE

Attila J Mozer
University of Wollongong
74 PUBLICATIONS **2,372** CITATIONS
SEE PROFILE

Pawel Wagner
University of Wollongong
105 PUBLICATIONS **1,726** CITATIONS
SEE PROFILE

Significant Performance Improvement of Porphyrin-Sensitized TiO_2 Solar Cells under White Light Illumination

K. Wagner,[†,‡] M. J. Griffith,[†] M. James,[§,||] A. J. Mozer,[†,‡,*] P. Wagner,[†] G. Triani,[§] D. L. Officer,[†,*] and G. G. Wallace[†]

ARC Centre of Excellence for Electromaterials Science, Intelligent Polymer Research Institute, University of Wollongong, Innovation Campus, Squires Way, Fairy Meadow, NSW 2519, Australia, Australian Nuclear Science and Technology Organisation (ANSTO), Locked Bag 2001, Kirrawee DC, NSW 2232, Australia, School of Chemistry, University of New South Wales, Sydney, NSW 2052, Australia, and Cooperative Research Centre for Polymers, 8 Redwood Drive, Notting Hill, VIC 3168 Australia

Received: August 12, 2010; Revised Manuscript Received: November 1, 2010

A significant improvement in the photovoltaic performance of porphyrin-sensitized TiO_2 solar cells under white light illumination is reported. The most significant improvement occurs within the first hour of light exposure and is irreversible within at least the studied 3-month period. Heat treatment in the dark produced only moderate performance improvement, whereas light treatment using a UV long-pass filter (>475 nm) led to an improvement similar to that obtained with the full simulated AM 1.5 spectrum, suggesting that the effect is linked to the photoexcitation of the porphyrin dye molecules. Light exposure resulted in simultaneous improvements in the short-circuit current (J_{sc}), the open-circuit voltage (V_{oc}), and the fill factor (FF). The J_{sc} improvement is attributed to better charge injection demonstrated by thin-film APCE measurements. Photovoltage decay measurements showed a factor of 2−3 increase in the electron lifetime after light exposure, accompanied by a comparable decrease in the electron diffusion coefficient. The improved electron lifetime combined with the increased J_{sc} resulted in increased electron densities under open-circuit conditions, leading to improved V_{oc}. Electrochemical impedance measurements showed a reduced charge-transfer resistance for I_3^- reduction at the Pt counter electrode, which is thought to be responsible for the increased filling factor. Furthermore, ATR-FTIR and X-ray reflectometry measurements indicated no significant change in the dye layer morphology after light exposure. An alternative mechanism involving the photogeneration of electronic states within the band gap of TiO_2 leading to improved injection, slower electron transport, and improved electron lifetime is discussed.

Introduction

Dye-sensitized solar cells (DSSCs)[1] utilize photoinduced charge injection from the photoexcited state of a sensitizing dye into the conduction band of a wide-band gap semiconductor, such as TiO_2, ZnO, or SnO_2. The efficiency of this charge separation step has been shown to be nearly 100%.[2] The inverse of this process, in which electrons are injected from the valence band of dye-sensitized photocathodes into the highest occupied molecular orbital (HOMO) of the photoexcited dyes with efficiency close to 100% has also been demonstrated, opening up further possibilities for organic dyes.[3] Porphyrins were one of the first sensitizers employed for dye-sensitized light-harvesting applications[4] and have remained among the most frequently studied dyes.[5] Their synthesis is relatively straightforward, and their optical and electronic properties can be tuned through chemical modification of the porphyrin core,[6] the number of porphyrin units,[7] and the linker between the core and the inorganic oxide.[8] Since we reported the then highest-efficiency porphyrin DSSC (7.1%) in 2007, a variety of new porphyrin dyes of comparable efficiency have been developed.[9,10] The development of new porphyrin dyes has been accompanied by a much-improved understanding of the photophysics in operational solar cells. For example, we showed in a series of benzoic-acid-linked Zn and free-base porphyrins that the luminescence lifetime, indicative of charge injection, depends not only on the driving force for injection but also on the conjugation through the linker moiety.[6] Furthermore, we showed that the electron lifetime in two of the most efficient porphyrin-sensitized solar cells is an order of magnitude lower than that in identically prepared ruthenium bipyridyl- (N719-) sensitized solar cells.[11] A phosphinic acid post-treatment of the porphyrin-sensitized solar cells led to an improved short-circuit current and electron lifetime.[12]

Herein, we report a significant performance improvement of porphyrin-sensitized TiO_2 solar cells under white light illumination. The effect is distinguished from smaller improvements observed due to heating of the samples in the dark. A combination of experimental techniques, including thin-film absorbed photon-to-current conversion efficiency (APCE) measurements, transient absorption spectroscopy (TAS), stepped light-induced measurements of photocurrent and photovoltage (SLIM-PCV), electrochemical impedance, and charge extraction techniques are employed to investigate the simultaneous improvement in the short-circuit current, open-circuit voltage, and fill factor. The light exposure effect provides a way to significantly and irreversibly improve solar cell efficiency. Moreover, it creates the opportunity to study some of the most fundamental limiting factors of porphyrin-sensitized solar cells.

* Corresponding author. E-mail: attila@uow.edu.au; davido@uow.edu.au.
[†] University of Wollongong.
[‡] Cooperative Research Centre for Polymers.
[§] Australian Nuclear Science and Technology Organisation (ANSTO).
[||] University of New South Wales.

10.1021/jp107615h
Published on Web 12/15/2010

A light exposure effect has been reported for various dye-sensitized systems. Wang et al. reported the redistribution of localized states within the TiO_2 conduction band leading to a conduction-band (CB) shift of the TiO_2 in solar cells sensitized with ruthenium bipyridyl complex Z907.[13] The improvement in efficiency, depending on the electrolyte used, was only moderate. Gregg et al. reported a significant (45-fold) increase in the performance of perylene-sensitized DSSCs upon exposure to UV light, which was also explained by a shift of the CB of TiO_2 and improved injection.[14] In this case, the V_{oc} decreased slightly. In the following year, the same authors concluded that the photoproduction of surface states by UV illumination might improve the injection efficiency and reduce recombination.[15] Mishra et al. showed a 30% improvement in the power conversion efficiency of dendritic oligothiophene ruthenium sensitizers after 12 days of light soaking at 60 °C and 1 sun.[16] Large improvements in both J_{sc} and V_{oc} were observed. Based on a red shift of the spectral response of the solar cells, the authors suggested the possible rearrangement of the thiophene unit under the light soaking conditions.

From the above studies, it is clear that the behavior of DSSCs upon prolonged light exposure is dye-dependent. The significant and simultaneous improvement in all device parameters of porphyrin-sensitized solar cells, reported here for the first time, suggests a complex phenomenon. We have systematically investigated the important photophysical pathways including charge injection, dye regeneration, charge recombination, and I_3^- recycling at the Pt counter electrode. We also confirmed that the effect cannot be explained by UV exposure alone. Attenuated total reflection Fourier transform infrared (ATR-FTIR) studies using the Australian synchrotron infrared microspectroscopy beamline did not show any effect on the binding mode of the dye to TiO_2. Finally, X-ray reflectometry measurements suggest no change in the dye layer thickness in planar structures comprising TiO_2/porphyrin heterojunctions grown by atomic later deposition (ALD), suggesting that morphological changes, if any, are minor.

Experimental Methods

Materials. Porphyrin dye GD2 [(*E*) 3-(5,10,15,20-tetra(3,5-dimethylphenyl)porphyrin-2-yl)propenylidenemalonato zinc (II)] was prepared as reported in ref 5c. The di(tetrabutylammonium salt) of GD2 was prepared by titration of GD2 with tertabutylammonium hydroxide. The model malonic acid used for the FTIR studies, (*E*) 3-(4-dimethylaminophenyl)propenylidenemalonic acid, was prepared by base-catalyzed condensation of malonic acid with 4-(dimethylamino)cinnamaldehyde, as described in the Supporting Information.

DSSC Fabrication. TiO_2 films were prepared on fluorine-doped tin oxide substrates (Asahi, $R_s \leq 8\ \Omega\ sq^{-1}$) using a doctor-blade technique. DSSCs shown in Figure 1 were prepared using a 5-μm transparent layer (Nanoxide-T, Solaronix), followed by a second 4-μm scattering layer (Nanoxide-300, Solaronix). DSSCs shown in Figure 2, as well as for TAS, SLIM-PCV, charge extraction, electrochemical impedance, and ATR-FTIR measurements consisted only of the transparent layer with 4−5-μm thickness. All film thicknesses were measured using a Dektak 150 profilometer. Thin (~2-μm) TiO_2 films for IPCE/APCE measurements were prepared by adjusting the spacer layer used in the doctor-blade technique. The TiO_2 films were sintered stepwise using a programmable hot plate with a maximum temperature of 500 °C. Each film was reheated to 450 °C before immersion into 0.2 mM anhydrous tetrahydrofuran solutions of porphyrin dye GD2 for 2 h. Sandwich-type

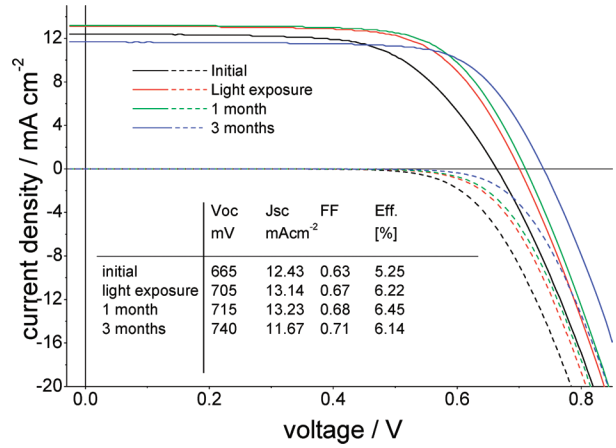

	Voc mV	Jsc mAcm^{-2}	FF	Eff. [%]
initial	665	12.43	0.63	5.25
light exposure	705	13.14	0.67	6.22
1 month	715	13.23	0.68	6.45
3 months	740	11.67	0.71	6.14

Figure 1. Current density−voltage curves measured for porphyrin-sensitized TiO_2 solar cells under AM 1.5 solar illumination (solid lines) and in the dark (dashed lines). Devices were tested as prepared (black), following 1 h of light exposure (red), and after 1 month (green) or 3 months (blue).

DSSCs were assembled using a 25-μm Hymilan sealant and Pt-sputtered (~8-nm thickness) indium tin oxide (ITO)−glass counter electrodes (Delta Technologies, $R_s \leq 10\ \Omega\ sq^{-1}$). An electrolyte solution composed of 0.6 M 1,2-dimethyl-3-propylimidazolium iodide (DMPII), 0.5 M 4-*tert*-butylpyridine, 0.1 M LiI, and 0.05 M I_2 in a solvent mixture of 85:15 acetonitrile/valeronitrile was injected between the electrodes through a hole in the counter electrode, which was subsequently sealed.

Light Exposure. Unless otherwise stated, light exposure refers to illumination of the DSSCs by 100 mW cm^{-2} simulated AM 1.5 light source at open circuit for 1 h. The temperature of the solar cells during this treatment was not controlled. After this treatment, the DSSCs were kept in the dark between the current−voltage measurements in Figures 1 and 3.

DSSC Characterization. Current−voltage curves were recorded using a Keithley 2400 source measure unit by illuminating the DSSCs with a simulated 100 mW cm^{-2} AM 1.5 light source (Oriel), calibrated using a certified Si diode equipped with a KG5 filter (Peccell). The device area was masked with black paint defining an aperture slightly larger than the active area.[17] Incident photon-to-current conversion efficiency (IPCE) spectra were recorded using a home-built setup consisting of a xenon lamp and a monochromator equipped with sorting filters. The light was focused onto a spot smaller than the DSSC area. The short-circuit current response of the devices was recorded in 5-nm steps using a Keithley 2400 source measure unit and referenced to the response of a calibrated silicon diode (Peccell).

APCE Measurements. Absorbed photon-to-current conversion (APCE) efficiency spectra were calculated as IPCE/LHE, where LHE is the light-harvesting efficiency of the dye-sensitized films. The absorbance of the dye-sensitized films used for LHE calculation was measured in transmission mode using a Shimadzu UV−vis 3600 spectrophotometer fitted with an ISR-3100 integrating sphere. Microscope cover slides were placed over the sensitized films, and an 85:15 acetonitrile/valeronitrile solution mixture was injected under the slide to ensure refractive indexes matched device conditions. A published optical model[18] was used to compute the LHEs of the dyes.

SLIM-PCV Measurements. Stepped light-induced measurements of photocurrent and photovoltage[19] (SLIM-PCV) were performed using a 635-nm diode laser illuminating the entire DSSC active area. Photocurrent and photovoltage transients were induced by stepwise small (≤10%) changes in the laser intensity. The electron densities at identical laser illumination intensities

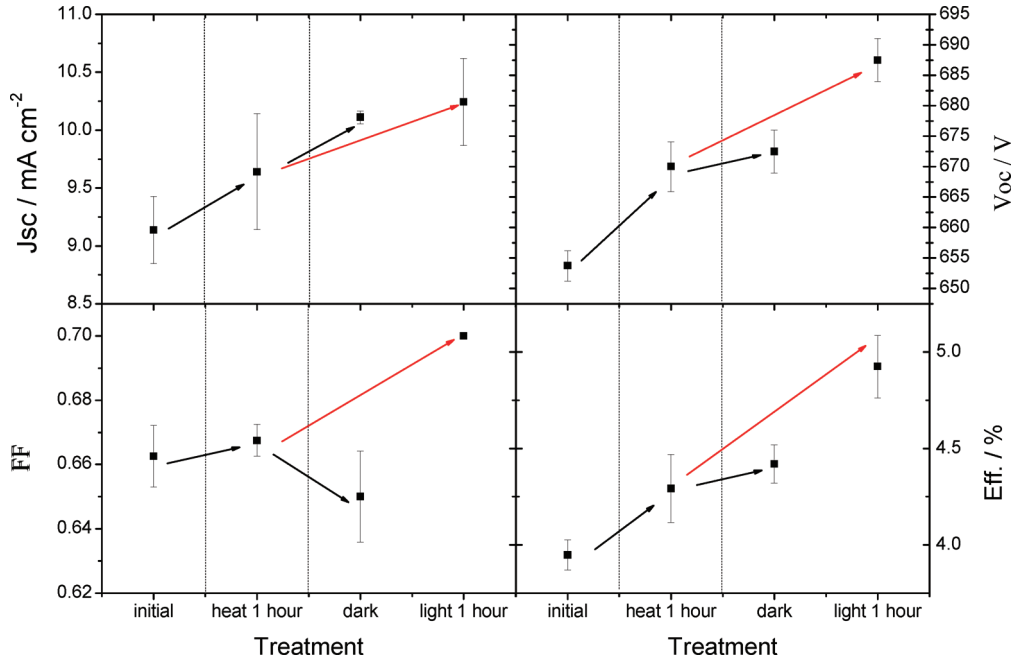

Figure 2. Short-circuit current density (J_{sc}), fill factor (FF), open-circuit voltage (V_{oc}), and power conversion efficiency of four DSSCs immediately after preparation and after samples had been kept at 60 °C for 1 h in the dark (heat 1 hour). Two samples were remeasured after being kept in the dark (dark), and another two were exposed to light for 1 h (light 1 hour). The symbols indicate the average values, and the error bars represent the standard variations.

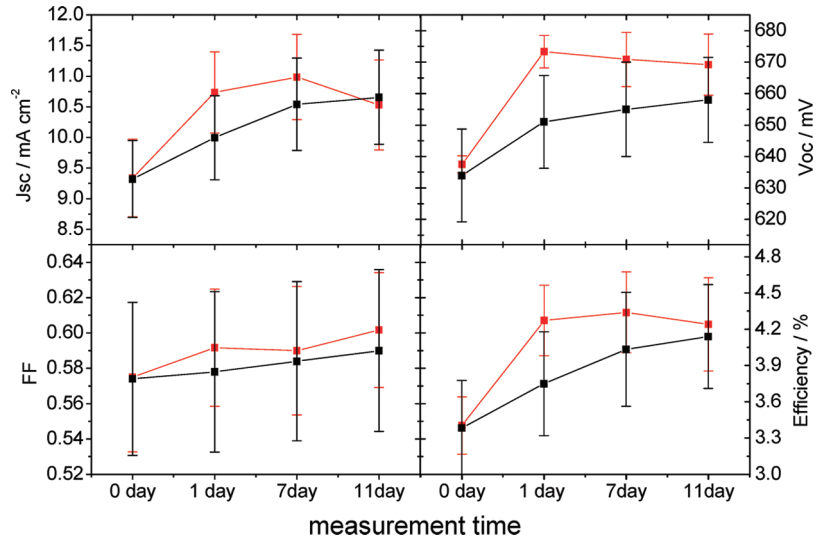

Figure 3. Short-circuit current density (J_{sc}), fill factor (FF), open-circuit voltage (V_{oc}), and power conversion efficiency of DSSCs immediately after preparation (day 0) and on days 1, 7, and 11. Red symbols indicate samples that were exposed to light for 1 hour between day 0 and day 1, whereas black symbols represent samples that were not. The symbols indicate average values, and the error bars represent the standard variations of six devices.

were determined by a charge extraction method[20] in which the light intensity was switched off at the same time the DSSC was switched from open to short circuit. The resulting current was integrated, with the electron density calculated from the amount of charge extracted.

Transient Absorption Spectroscopy. Transient absorption kinetic traces were acquired by photoexciting the dye-sensitized TiO_2 films through the fluorine-doped tin oxide (FTO)/TiO_2 surface by the nanosecond pulses of a Q-switched Nd:YAG (Indi, Spectra Physics) laser and monitoring the change in the transmission of a probe beam at 700 nm using a photoreceiver (Femto) and a Tektronix oscilloscope (nominal combined bandwidth of 200 MHz). A xenon lamp and a band-pass filter (40 fwhm) before the sample and a monochromator and a 532-nm notch filter after the sample were used as a probe. The pump laser repetition rate was 10 Hz; measurements performed at 1 Hz showed no difference in the kinetics.

Electrochemical Impedance Spectroscopy (EIS). Electrochemical impedance measurements were recorded by illuminating the DSSCs with 100 mW cm^{-2} calibrated AM 1.5 illumination at open-circuit conditions between 0.1 Hz and 100 kHz with an AC amplitude of ±10 mV using a Gamry Reference 600 instrument. Spectra were analyzed and fitted using ZView version 3.0.

FTIR Characterization. Infrared spectra were collected for sensitized TiO_2 films obtained by disassembling devices once the performance enhancement effect induced by light exposure had been verified through current-density−voltage ($J-V$) curve measurements. The films were analyzed using a Bruker Vertex V80 v FTIR spectrometer coupled with a Hyperion 2000

microscope equipped with a liquid-nitrogen-cooled narrow-band mercury cadmium telluride (MCT) detector at the Australian Synchrotron infrared microspectroscopy beamline. Samples were measured using attenuated total reflection (ATR) mode with a 100 μm germanium crystal. Spectra were acquired with OPUS 6.5 software using a 20 × 20 μm aperture with 256 coadded sample scans per film and 256 coadded background scans after every 3−5 samples. A resolution of 2 cm^{-1} was employed for all sample and background measurements.

X-ray Reflectometry. Conformal TiO_2 layers were deposited using atomic layer deposition (ALD). Self-limiting surface-mediated reactions of $TiCl_4$ and H_2O were used to deposit a TiO_2 film of 10 nm nominal thickness onto a Si⟨100⟩ wafer using an F-120 ALCVD reactor from ASM Microchemistry. The deposition temperature (200 °C) and pulsing conditions were chosen to produce a planar layer with low surface roughness.[21] X-ray reflectivity spectra were measured on a Panalytical Ltd. X'Pert Pro Reflectometer using Cu Kα X-ray radiation (λ = 1.54056 Å). The X-ray beam was focused using a Göbel mirror and collimated with 0.2-mm pre- and postsample slits. Reflectivity data were collected over the angular range of $0.05° \leq \theta \leq 5.00°$, with a step size of 0.010° and a counting time of 10 s per step. X-ray reflectivity data were collected on freshly prepared TiO_2 films with no dye coating, as well as on the same surfaces after they had been soaked in dye. Structural parameters associated with layers within these films were refined using MOTOFIT,[22] with X-ray reflectivity data plotted as a function of momentum transfer normal to the surface [$Q = 4\pi(\sin\theta)/\lambda$)]. Initial structural models were prepared using estimated values of the X-ray scattering length density (SLD) of 3 × 10^{-5} $Å^{-2}$ for the TiO_2 film and 1 × 10^{-5} $Å^{-2}$ for dye layers. A native silicon oxide layer was not included in these structural models, as little contrast was present between the SLD of the Si wafer (2.0 × 10^{-5} $Å^{-2}$) and that of the native oxide (1.9 × 10^{-5} $Å^{-2}$). In the structural model, the thickness, SLD, and interfacial roughness of each layer were refined, and the Levenberg−Marquardt method was used to minimize χ^2 values.

Results

In this study, porphyrin-sensitized solar cells were prepared using standard procedures, and their current−voltage characteristics were immediately recorded. The solar cells were then subjected to 1 h of light exposure (100 mW cm^{-2} simulated AM 1.5), and the current−voltage characteristics were remeasured. The current−voltage characteristics measured after device fabrication (black), remeasured after 1 h of light exposure (red), and 1 (green) or 3 (blue) months after fabrication are shown in Figure 1. Solid lines indicate measurements under illumination, whereas dashed lines indicate measurements performed in the dark. The DSSC was kept in the dark between measurements. Immediately after sample preparation, the DSSC exhibits a short-circuit photocurrent density (J_{sc}) of 12.4 mA cm^{-2}, an open-circuit voltage of (V_{oc}) 665 mV, and a fill factor of 0.63, which corresponds to a power conversion efficiency of 5.3%. After 1 h of light exposure, the J_{sc} increased to 13.1 mA cm^{-2} (6% improvement), accompanied by an additional 6% increase in both V_{oc} and FF, leading to a 6.2% efficiency. The efficiency further improved to 6.5% after 1 month because of improvements in V_{oc} and FF and slightly decreased after 3 months because of a drop in J_{sc}, which was not compensated by a rather significant increase in the V_{oc}. The current density−voltage characteristics of the devices without illumination indicate a current onset of approximately 0.5 V directly after assembly. This onset shifted to around 0.6 V following 1 h of light exposure and remained similar over the 3-month period.

Next, we measured the photovoltaic parameters of four identically prepared DSSCs initially and after 1 h of exposure to 60 °C in the dark (Figure 2). Two of these "heat-treated" samples were then further exposed to light for 1 h, whereas the other two were kept in the dark. On average, a 9% increase in the solar cell efficiency was observed after heat treatment, with similar increases in J_{sc}, V_{oc}, and FF. This improvement combines possible changes due to brief light exposure during the initial photovoltaic (PV) measurements lasting for 2 min and any additional changes due to exposure to 60 °C in the dark. In comparison, the two samples kept in the dark also improved slightly, presumably because of exposure to light during the PV measurement step. This improvement is similar to what we observed below, where the long-term performance of two sets of devices with and without 1 h of exposure to light was monitored. Importantly, the efficiency showed further significant improvements when two of the heat-treated samples were subsequently exposed to light for 1 h, indicating that the possible effect of elevated temperatures is not the main reason for the performance improvement of porphyrin-sensitized TiO_2 solar cells. All of the main parameters were improved significantly during this light-exposure step.

The reproducibility of the observed improvements and the long-term behavior of the DSSC performance were monitored over 11 days, as shown in Figure 3. These samples contained only a relatively thin (5 μm) transparent TiO_2 layer; therefore, the efficiencies were lower than in Figures 1 and 2, for which the data were collected from devices containing a combination of transparent and light-scattering TiO_2 layers. The performance of six identically prepared samples was monitored immediately after fabrication and subsequently 1, 7, and 11 days after fabrication (black). Six further samples were exposed to light after the initial measurement for 1 h (red) and were then remeasured after identical time periods. All samples were kept in the dark between measurements. Despite a noticeable variation in the initial performance of the devices, the samples exposed to light for 1 h showed a significant improvement (average of 26%), which remained relatively constant with a slight drop in J_{sc}, V_{oc}, and efficiency on days 7 and 11. In contrast, the devices that were not exposed to specific light treatment displayed a gradual improvement in performance over the 11-day measurement period, likely as a result of light exposure during each of the measuring steps lasting approximately 2 min. The average efficiency of these "dark" devices showed a total improvement of 11% after the first measurement and 23% after 11 days. Each photovoltaic test increased the performance of the devices. We note that the improvement observed after the first PV test (between day 0 and day 1) was similar to that observed in Figure 2 for the samples exposed to only heat after the initial measurement, suggesting that the main improvement in both cases was indeed due to brief exposure to light rather than the 1 h of exposure to elevated temperature.

We also compared the performance of two identically prepared DSSCs containing only a transparent TiO_2 layer (i) exposed to only the visible part of the solar spectrum by using a 475-nm long-pass filter, (ii) exposed to the full simulated AM 1.5 spectrum, and (iii) kept in the dark. The improvements in each of the parameters are compared to the average performance of six devices without any treatment applied (initial) in Table 1. These measurements indicate no significant difference between the samples exposed to the full simulated AM 1.5 spectrum or to the visible−IR region only. From all of the above experiments, we conclude the following:

TABLE 1: Photovoltaic (PV) Parameters of Porphyrin-Sensitized TiO_2 Solar Cells Exposed to (i) the Visible/Infrared Range and (ii) the Full Simulated AM 1.5 Spectrum for 1 h Compared to the Average Performance of the As-Prepared Devices and (iii) Those Kept in the Dark after the First PV Measurements, along with (iv) Average Value of Six Samples without Any Treatment Applied

treatment	V_{oc} (mV)	J_{sc} (mA/cm^2)	FF	η (%)
(i) VIS	635 (1%)	10.2 (36%)	0.67 (5%)	4.3 (43%)
	640 (1%)	9.3 (24%)	0.62 (−4%)	3.7 (23%)
(ii) AM 1.5	645 (2%)	8.4 (12%)	0.69 (8%)	3.7 (23%)
	650 (3%)	9.1 (21%)	0.68 (6%)	4.0 (33%)
(iii) dark	620 (−2%)	7.9 (5%)	0.64 (0%)	3.2 (6%)
	630 (0%)	7.9 (5%)	0.65 (1%)	3.2 (6%)
(iv) average initial	630 ± 9	7.5 ± 0.5	0.64 ± 0.02	3.0 ± 0.1

(1) The most significant improvements occurred within the first hour of light exposure. The changes were irreversible over the studied 3-month period. All photovoltaic parameters improved during light exposure.

(2) Heating of the samples in the dark cannot explain the full extent of the improvement in the performance.

(3) Exposure to only the visible−IR (>475 nm) region of the spectrum produced improvements of similar magnitude to those observed for exposure to the whole simulated AM 1.5 spectrum, indicating that direct photoexcitation of the porphyrin dye must play a role.

The long-term stability of DSSCs is a complex issue and might involve a combination of processes operating on different time scales, for example, absorption/desorption of the electrolyte components at the TiO_2 interface,[23] dye desorption,[24] electrolyte evaporation, and dye degradation.[25] Most of the improvements to the device performance occurred within the first hour. The decrease in the devices' performances, possibly due to any of the degradation mechanisms mentioned above, occurred on the longer time scale (4 days to 3 months). Therefore, in the rest of this study, we limited our focus to the changes observed within the first hour of light exposure.

Discussion

Light exposure of porphyrin-sensitized DSSCs has been shown above to produce substantial performance enhancements arising from the simultaneous improvement of V_{oc}, J_{sc}, and FF. We have probed several of the photophysical pathways in these DSSCs in order to elucidate the origin of these improvements. The various photophysical pathways in a typical dye-sensitized solar cell and the various characterization techniques that we used to probe them in this section are presented in Figure 4.

Charge Injection (A). The incident photon-to-current conversion efficiency (IPCE) combines contributions from the light-harvesting efficiency (LHE), the efficiency of electron injection from the photoexcited dye into the TiO_2 conduction band (ϕ_{inj}), and the efficiency of charge collection at the contacts (ϕ_{coll}), so that IPCE = LHE$\phi_{inj}\phi_{coll}$. The absorbed photon-to-current electron efficiency (APCE) is APCE = IPCE/LHE = $\phi_{inj}\phi_{coll}$. In thin (2 μm) porphyrin-sensitized TiO_2 DSSCs, the mean diffusion length of electrons is larger than the electron lifetime;[11] therefore, at J_{sc} conditions, ϕ_{coll} is assumed to be close to 100%. IPCE measurements coupled to accurate LHE calculations consequently enable the determination of ϕ_{inj} under short-circuit conditions. We previously reported an optical model in which LHE in thin-film DSSCs is calculated using the absorbance of the dye-sensitized films and the electrolyte layer. In this model, we include the fraction of light absorbed following light reflection from the Pt counter electrode. In 2 μm porphyrin-sensitized DSSC devices, our calculation suggests that this corresponds to an increase of approximately 3−4% in the LHE at longer wavelengths (550−650 nm), where the dye molar extinction coefficient is smaller.

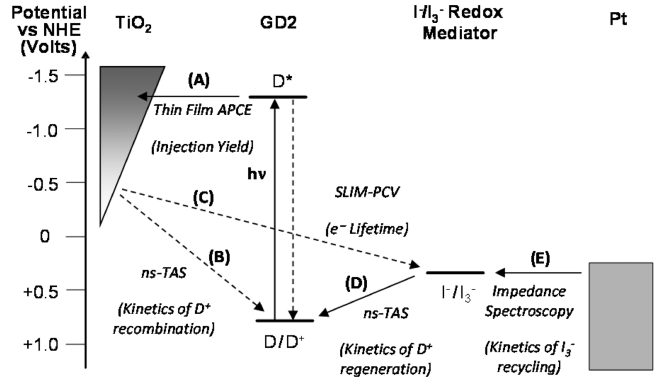

Figure 4. Schematic representation of the energy levels of a DSSC indicating the various competing photophysical pathways, including (A) electron injection, (B) electron recombination with dye cations, (C) electron recombination with the acceptor species in the electrolyte, (D) regeneration of dye cations by I^-, and (E) recycling of I_3^- at the counter electrode. The techniques used to probe each of these processes are also included.

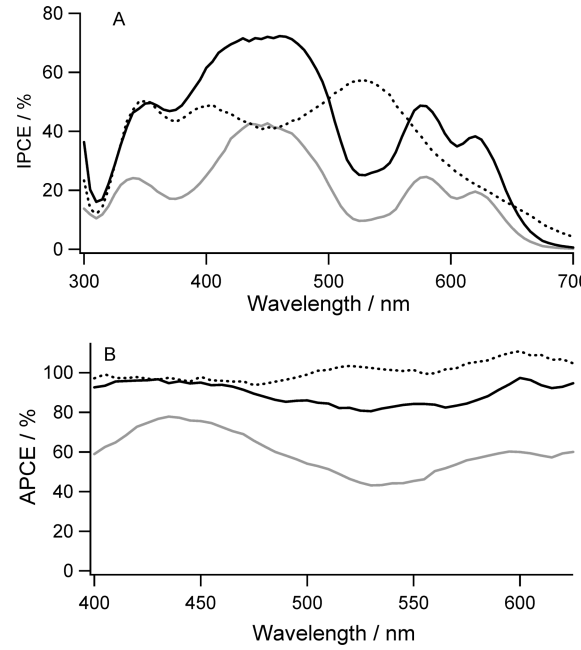

Figure 5. (A) Incident photon-to-current conversion efficiencies (IPCEs) and (B) absorbed conversion efficiencies (APCEs) for porphyrin-sensitized thin film TiO_2 devices before (gray solid line) and after (black solid line) 1 h of light exposure. Data for N719 dye is included for comparison (dashed line).

Figure 5A shows the IPCE of porphyrin-sensitized solar cells before and after 1 h of light exposure. A significant increase across the entire absorption spectrum of the dye was found, corresponding to a calculated 30% increase in J_{sc} when integrated with the AM 1.5 spectrum, which is comparable to what was observed in current-density−voltage measurements. A comparable increase in the IPCE was also observed using thicker (9 μm) TiO_2 films, suggesting that the film thickness does not influence the effect.

The APCE spectra, calculated as IPCE/LHE, are shown in Figure 5B. Because the LHE did not change after light soaking, the IPCE increase originates from the increased APCE (from

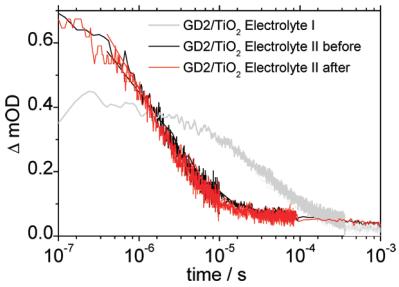

Figure 6. Transient absorption kinetic traces recorded at 700 nm in the absence (electrolyte I) and in the presence (electrolyte II) of I^-/I_3^-. Black and red lines, respectively, indicate decays recorded before and after the fully assembled solar cells had been exposed to white light for 1 h. The films were photoexcited by nanosecond pulses at 532 nm.

65% to approximately 90%) following light exposure. In comparison, APCE measurements of ruthenium bipyridyl- (N719-) sensitized solar cells showed values close to 100%, in agreement with previously published 100% charge injection yield for this dye under similar conditions. The light-induced enhancement of the porphyrin-sensitized films was uniform across a wide spectral range, indicating that charge injection improved independent of wavelength. This excitation wavelength independence can be explained by a fast relaxation of the photoexcited state and therefore electron injection mostly occurring from the lowest photoexcited state. We also note that, contrary to previous reports on dendritic oligothiophene ruthenium sensitizers, no shift in the dye absorption or IPCE spectra was observed upon light exposure.

Charge Recombination (B−D). The improved short-circuit current might also originate from faster dye regeneration of dye cations by I^- (process D in Figure 4) or from slower recombination between injected electrons and the electron-accepting I_3^- ions in the electrolyte (process C, Figure 4). Figure 6 shows kinetic transient absorption (TA) traces recorded at 700 nm. At this wavelength, the signal is dominated by photon absorption of porphyrin cations with contributions of photon absorption by subgap TiO_2 electrons. The porphyrin-sensitized TiO_2 films were photoexcited at 532 nm with approximately 30 μJ cm^{-2} per pulse energy. The samples either contained electrolyte I (0.1 M $LiClO_4$ in acetonitrile/valeronitrile) or were fully operational solar cells containing standard electrolyte II (0.6 M DMPII, 0.5 M 4-*tert*-butylpyridine, 0.1 M LiI, and 0.05 M I_2 in acetonitrile/valeronitrile). The TA trace at 700 nm in the absence of the redox mediator (electrolyte I) had a half-signal decay of around 60 μs, corresponding to the recombination reaction between dye cations and photoinjected electrons in the TiO_2 (process B in Figure 4). The signal decay accelerated in the presence of electrolyte II, which indicates regeneration of the dye cations by I^- ions with signal half-decays of around 2 μs. A second, smaller, long-lived component of the signal was also observed and attributed to the recombination of TiO_2 electrons with I_3^- ions. The fully assembled DSSC was then exposed to white light until an increase of approximately 25% in J_{sc} was observed. This procedure allowed us to keep the samples in the exact same position yet still confirm the characteristic improvement in J_{sc} due to the light-exposure effect. The dye regeneration kinetics did not change after the treatment, which suggests that the improvement in J_{sc} was not due to improved dye cation regeneration. This can also be rationalized from Figure 6, showing that, under these excitation conditions, more than 90% of the dye cations were regenerated within 10 μs. The dye cation signal decay was only minimal in the same period (<10%). We note that attempts to determine the effect of light exposure on

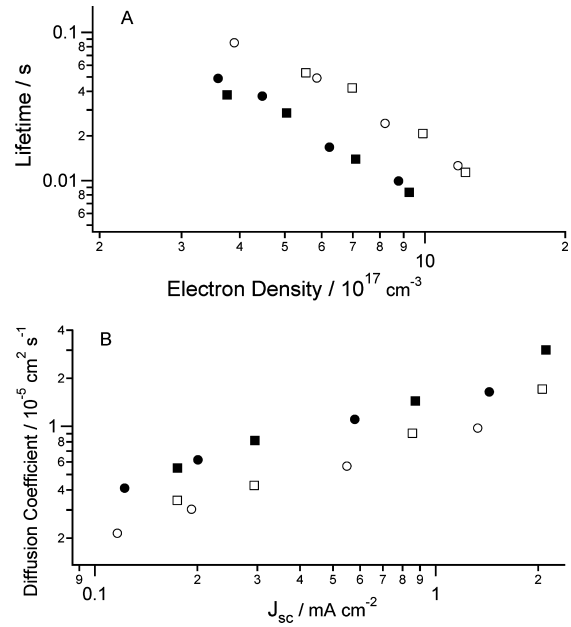

Figure 7. (A) Electron lifetime versus electron density and (B) electron diffusion coefficient versus short-circuit current density before (■,●) and after (□,○) 1 h of light exposure.

the dye cation−TiO_2 electron recombination in the absence of the I^-/I_3^- mediator (electrolyte I) were not successful because of degradation of the dye layer. This was confirmed by a significant color change (blue shift) of the porphyrin-sensitized film, accompanied by a considerable acceleration of the kinetic traces at 700 nm under 1 h of white light illumination.

Open-circuit voltage decays were measured for as-prepared and light-exposed porphyrin-sensitized DSSCs by illuminating them with a 635 nm diode laser. Electron lifetimes measured before and after 1 h of light exposure are shown for different laser intensities in Figure 7.

The electron lifetime after light exposure at matching electron density increased by a factor of 2−3. Although J_{sc} was found to increase slightly during illumination by the 635 nm laser, the measurements were not appreciably affected by light treatment by the laser illumination. This was confirmed by detecting only a small change in the as-prepared devices measured multiple times (not shown). The longer lifetimes measured for light-exposed devices suggest a reduced recombination rate between TiO_2 electrons and I_3^- ions in the electrolyte, which should be the dominating recombination reaction because of the efficient regeneration of dye cations by I^- as shown by TAS measurements. The reduced recombination rate between TiO_2 electrons and I_3^- is thought to be responsible for the increased dark-current onset (by approximately 100 mV) in Figure 1.

The diffusion coefficient of electrons in the TiO_2 was found to decrease after light exposure by a similar magnitude, which might explain the slower recombination in accordance with an electron-diffusion-controlled recombination model.[26] The slower electron diffusion might be related to an increased concentration of subgap states. Gregg et al.[15] and Grätzel et al.[13] previously suggested the photogeneration of such states by UV illumination. Overall, the charge extraction efficiency, determined by the mean electron diffusion length $l = (D\tau)^{0.5}$, where D is the diffusion coefficient and τ is the electron lifetime, and, as determined by SLIM-PCV, did not change after light exposure and was between 7 and 20 μm depending on the electron density. This also confirms that the improved APCE in 2 μm TiO_2 films

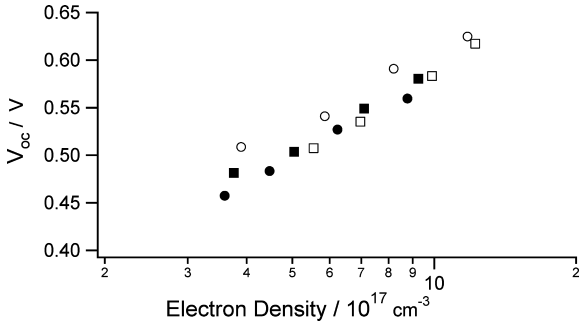

Figure 8. Open-circuit voltage versus electron density before (■,●) and after (□,○) 1 h of light exposure.

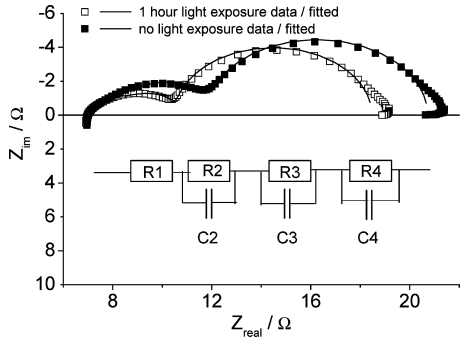

Figure 9. Nyquist plots of porphyrin-sensitized solar cells before (■) and after (□) 1 h of light exposure. The symbols represent measurement data, and the lines represent curves fitted to the equivalent circuit diagram displayed in the inset.

was due not to improvements in charge extraction, but rather to improved charge injection as demonstrated above.

V_{oc} versus electron density obtained by a charge extraction method is shown in Figure 8 for as-prepared and light-exposed samples. We did not observe a noticeable shift along the V_{oc} axis or any change in the slope of V_{oc} versus electron density using the standard electrolyte. Assuming that the redox potential of the I^-/I_3^- electrolyte solution does not change significantly under illumination, V_{oc} logarithmically depends on the ratio of electron density in the TiO_2 under illumination (N_{CB}^i) and in the dark (N_{CB}^d) as $V_{oc} \propto A \log(N_{CB}^i/N_{CB}^d)$. The V_{oc} versus electron density plot, indicative of the splitting of the quasi-Fermi levels at a given electron density, is therefore influenced by the distribution and concentration of the subgap electron trap states. The V_{oc} value at a given electron density also depends on the conduction-band potential of TiO_2, which is known to be sensitive to the additives used in the electrolyte. The lack of change in the V_{oc} versus electron density plot suggests that the CB potential of TiO_2 did not shift following light exposure. A combined effect, however, such as Li^+ ion desorption (negative shift) and increased trap concentration (positive shift) compensating for each other, cannot be ruled out. The origin of the improved V_{oc} value is therefore attributed to an increased electron density at the same illumination condition at open circuit, which is due to the combined effect of improved charge injection and reduced charge recombination.

I_3^- Recycling at the Counter Electrode (E). Figure 9 shows Nyquist plots obtained by electrochemical impedance measurements performed at V_{oc} conditions before and after 1 h of light exposure. The spectrum reveals three semicircles, represented by a series of three parallel RC circuit elements. Because of the nanoporous nature of DSSCs, their impedance spectra are typically fitted to an equivalent circuit model based on an infinite transmission line.[27] For simplicity, the experimental curves in Figure 9 were fitted to the equivalent circuit model displayed in the inset, and the fitted values are reported in Table 2. Similar to previous studies,[28] the first semicircle (R_2-C_2), corresponding to a frequency range of approximately 400−25 kHz, is attributed to charge-transfer resistance at the FTO/TiO_2 interface and was unchanged after light exposure. In contrast, the second (R_3-C_3, 25−1 kHz) and third (R_4-C_4, 1 kHz to 10 Hz) semicircles, attributed to charge-transfer resistance at the platinum-coated counter electrode and the TiO_2/dye/electrolyte interface, respectively,[16,29,30] changed noticeably. Following light exposure, charge-transfer resistance at both the platinum counter electrode and the TiO_2/porphyrin/electrolyte interface decreased. This result indicates that the observed performance enhancement involved both interfaces. The decreased charge-transfer resistance at the TiO_2/porphyrin/electrolyte interface is attributed to an increased electron density in the TiO_2 at the same illumination conditions, which is due to increased charge injection and reduced charge recombination as discussed above. Electron lifetimes were calculated from phase shift versus frequency plots as $1/f_{RC_3}$, where f_{RC_3} is the frequency at which the phase shift is maximum for the R_3C_3 semicircle. The calculated values are 12.5 ms before and 15.9 ms after 1 h of light exposure. The measured increase in electron lifetime is slightly less than the SLIM-PCV results. The V_{oc} value before light exposure at 100 mW cm^{-2} illumination was 603 mV, which increased to 625 mV after light exposure, indicating that the electron density has increased. As shown in Figure 7A, the increased electron density after light exposure at the same illumination intensity leads to reduced lifetime, which at least partially explains the smaller increase in electron lifetime measured by EIS compared to SLIM-PCV.

The decrease in charge-transfer impedance at the platinum-coated counter electrode over time was reported by Grätzel et al. for N719-sensitized devices exposed to 2 days of thermal aging.[16] The decrease was attributed to either the activation of the platinum electrocatalyst or an improvement in the contact between the electrolyte and platinum. The reduced charge-transfer resistance induced an increase in the device fill factor of the DSSCs. We note that we used a relatively flat 8 nm platinized counter electrode prepared by a sputtering technique; therefore, an improvement in the surface area of the Pt catalyst layer due to dissolution of Pt, for example, would also explain the above changes. We showed recently a similar reduction in the charge-transfer resistance at the platinum/electrolyte interface by using a controlled electrodeposition technique leading to nanostructured platinum deposits with an increased surface area.[31] Similarly to ref 16, we propose that the improvement in the FF has a significant contribution from the reduced charge-

TABLE 2: Resistance (R) and Capacitance (C) Values Obtained by Fitting the Equivalent Circuit Displayed in the Inset of Figure 9 to the Electrochemical Impedance Data Obtained at V_{oc} and 100 mW cm^{-2} Simulated AM 1.5 Sunlight Illumination before and after 1 Hour Light Exposure of Porphyrin-Sensitized TiO_2 Solar Cells[a]

	R_1 (Ω)	R_2 (Ω)	C_2 (F)	R_3 (Ω)	C_3 (F)	R_4 (Ω)	C_4 (F)
before	7.1 (0.4%)	1.5 (6.1%)	3.2×10^{-6} (5.6%)	3.2 (2.9%)	1.2×10^{-5} (6.8%)	8.8 (0.9%)	2.9×10^{-4} (1.8%)
after 1 h of light exposure	7.1 (0.3%)	1.5 (6.0%)	3.2×10^{-6} (5.0%)	2.0 (4.5%)	1.7×10^{-5} (10%)	7.9 (0.8%)	3.8×10^{-4} (1.5%)

[a] Estimated error given by the fitting algorithm for each parameter in parentheses.

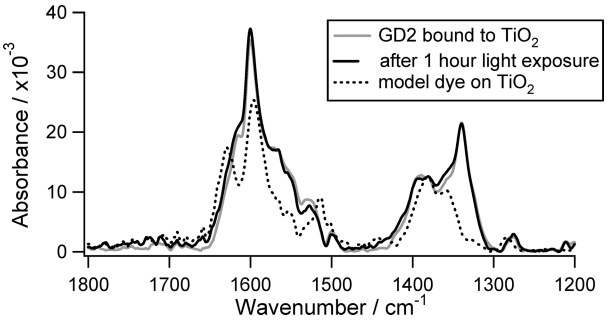

Figure 10. Carboxylate region of the ATR-FTIR spectrum recorded for porphyrin-sensitized TiO_2 films before (gray solid line) and after (black solid line) 1 h of light exposure. The analogous spectrum for the model dye adsorbed to TiO_2 (dashed line) is also displayed.

transfer resistance at the counter electrode. We note that, whereas most of the improvement in J_{sc} and V_{oc} occurred after 1 h of light exposure, the increase in FF was gradual over the 11-day period (Figure 3). Moreover, the improvements in the FF with or without light exposure over 11 days were quite similar, indicating that a different process, such as changes to the morphology of the platinum layer, might be operating.

Two main mechanisms have been reported to date to explain the improved J_{sc} and V_{oc} values of DSSCs under prolonged illumination. The first involves the rearrangement of the dye molecules, leading to better electronic coupling or reduced aggregation.[14] The second mechanism involves the photogeneration of subgap states that improve charge injection and charge transport.[13,15,16] The latter was based on a prediction that a percolation threshold for intertrap hopping can be reached at higher concentrations.[15]

The lack of spectral shift in the porphyrin absorption upon light exposure indicated no major molecular reorganization or aggregation-induced effect. To study this further, we probed the attachment of the dye at the TiO_2 surface by studying the IR bands of the characteristic binding modes. Given the dicarboxylic acid binder present on the GD2 dye molecule, several different TiO_2 binding modes and resulting orientations are possible. As discussed by Srinivas et al., either one or both carboxylic acids could bind in either ester-like monodentate binding in which one carboxylate oxygen forms a single oxygen metal bond or bidentate bonding in which each carboxylate oxygen binds to a single metal atom (chelating) or to two separate metal atoms (bridging).[32] They dismissed the possibility of both carboxylic acid groups binding at the same time in a bidentate bridging mode, however, as being too strained; this would only be true on a flat surface, and this mode of binding could occur at TiO_2 particle edges and interfaces where there were appropriately placed Ti atoms. In addition, where only one carboxylic acid is bound, the second free acid could be protonated or dissociated depending on its environment. These various binding modes could lead to different coupling and dye/TiO_2 distances, affecting both injection and recombination kinetics.

The carboxylate binding modes of the GD2 dye were investigated by recording the ATR-FTIR spectra acquired on sensitized films on the IR microspectroscopy beamline at the Australian Synchrotron (Figure 10). Comparison was made to a small-molecule dye with an analogous malonic acid binding group, 2-carboxy-5-(4-(dimethylamino)phenyl)penta-2*E*,4*E*-dienoic acid, in order to determine the bound-dye CO symmetric and asymmetric stretches. In addition, the di(tetrabutylammonium salt) of GD2 was analyzed because it is well-established that the difference between the asymmetric and symmetric COO^- bands in the ionic and adsorbed states can be used as a criterion to differentiate between monodentate and bidentate binding.[5b,33]

As shown in Figure 10, the binding modes were determined by a comparison of the FTIR bands of the model dye bound to TiO_2 with those of GD2 in the carboxylate region of the spectrum. The GD2 bands at 1610 and 1388 cm^{-1} are identified as the asymmetric and symmetric COO^- stretching peaks, respectively, and no carbonyl bands arising from free carboxylic acids are evident. The intense peak at 1600 cm^{-1} is attributed to C═C stretches, although, as observed in previous porphyrin dye spectra,[5b,34] this band is typically sharp. Therefore, it is likely that there is more than one type of COO^-_{asym} stretch contributing to the broadness of the band around 1600 cm^{-1}. Comparison of this spectrum with that of the GD2 free salt (Figure S1, Supporting Information) revealed a smaller spacing between the two COO^- stretching peaks for the dye-adsorbed sample (222 cm^{-1}) than for the free salt (261 cm^{-1}). This, together with evidence that the chelation mode is unstable, suggests that GD2 is bound to the TiO_2 by a bridging bidentate binding mode as shown in Figure S2a (Supporting Information). However, given the breadth of the bands around 1600 cm^{-1} as discussed above, it is likely that there are different bridging bidentate binding modes involving either one or both carboxylate groups, as illustrated by Srinivas et al.,[32] with any free carboxylate in the dissociated form.

Furthermore, as is evident in Figure 10, no differences in the binding modes of the dye for as-prepared and light-exposed samples were detected. The films were acquired by disassembling working DSSC devices. The light exposure effect was verified by current−voltage measurements prior to acquiring the IR spectra. The penetration depth of the IR beam was estimated to be ~1 μm. This result therefore suggests that there was no noticeable change in the chemical attachment of the dyes at least within this top 25% region of the dye-sensitized film. Changes to the dye binding modes closer to the FTO surface, however, cannot be ruled out.

To gain further insight into the binding of GD2 on TiO_2 and whether it is affected by light exposure, the thickness of the dye layer on a planar ALD-grown TiO_2 surface before and after light exposure was investigated using X-ray reflectometry. From the thickness, the main orientation of dye molecules can be established. As discussed above, the molecular orientation of the sensitizing dye can have a large impact on the injection and recombination in DSSC devices, for example, by altering the overlap of excited state orbitals with the TiO_2 3d orbitals affecting charge injection or by creating dye layers of varying thickness and density, which could influence electron recombination in TiO_2 with I_3^-.[35] For these measurements, a TiO_2 layer was deposited onto a silicon wafer by atomic layer deposition. This produced a conformal TiO_2 surface (with rms surface roughness, $R < 0.4$ nm), which is required for this type of analysis. X-ray reflectivity spectra for the ALD-grown TiO_2 substrate (red data points) and the porphyrin-sensitized TiO_2 before (blue data points) and after (green data points) light exposure are shown in Figure 11.

The TiO_2 substrate was accurately modeled using a single-layer approach, with the TiO_2 layer determined to be 8.1(1)-nm thick and having a surface roughness of 0.4(1) nm. The refined scattering length density (SLD = 3.1×10^{-5} $Å^{-2}$) reveals that the titania film had a mass density of 3.86 g/cm^3, 0.99% of the value for crystalline anatase.[21] In contrast, X-ray reflectivity data from the as-prepared porphyrin-sensitized film could not

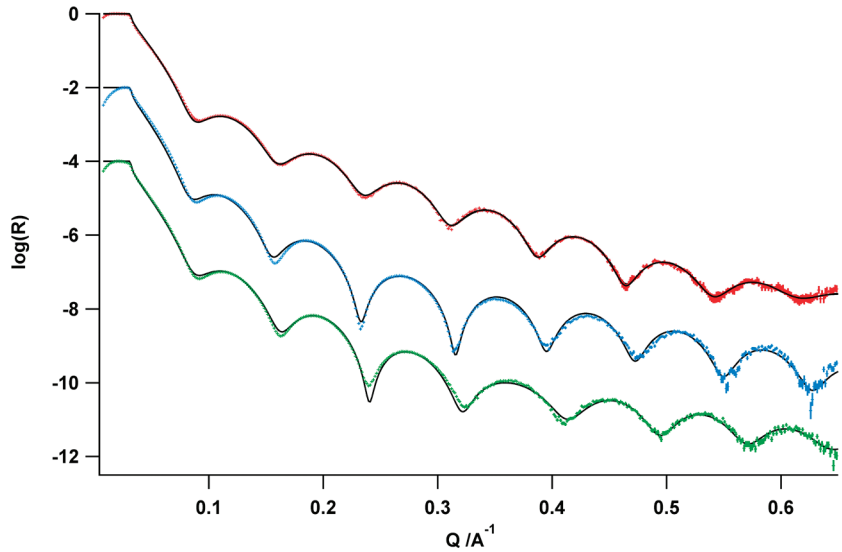

Figure 11. Observed (data points) and calculated (solid lines) X-ray reflectivity spectra for a TiO_2 substrate (red data points) and porphyrin-sensitized TiO_2 before (blue data points) and after (green data points) 1 h of light exposure.

be modeled by a single layer, but rather required a two-layer model. The base layer of this film is TiO_2 [8.0(1) nm], with a refined SLD of 3.1×10^{-5} Å^{-2} and an interfacial roughness of 0.3(1) nm. The upper layer (the porphyrin dye) was found to be 1.0(1)-nm thick after rinsing with acetonitrile, with an SLD of 1.0×10^{-5} Å^{-2} and a surface roughness of 0.4(1) nm. This dye thickness is consistent with the molecular size of a GD2 (18 Å) and indicates that the dye was adsorbed to the TiO_2 at an angle of ~23° with respect to the plane of the substrate surface (see model in Figure S2b, Supporting Information). The porphyrin-sensitized film was then subjected to light exposure using a halogen lamp equipped with an infrared cutoff filter to avoid excess heating and solvent evaporation, while covered in standard iodide/triiodide redox electrolyte. The fitted X-ray reflectivity spectra obtained after light exposure displayed negligible changes to both the calculated dye layer density (0.9×10^{-5} Å^{-2}) and thickness [0.9(1) nm]. This result indicates that the orientation of the dye layer on the TiO_2 surface was unaffected by light exposure. The question of whether these results obtained on flat TiO_2/dye heterojunctions are directly applicable to mesoporous TiO_2 films remains to be answered. Nevertheless, none of the above experiments suggest a change in the optical absorption, the binding mode, or the dye layer thickness. This implies that the significant improvement to the photovoltaic performance is not due to morphological changes of the dye layer.

The reduction in diffusion coefficient by a factor of 2−3 upon light exposure might originate from the photogeneration of subgap electron trap states as postulated by Gregg et al.[13] and Grätzel et al.[15] The lack of change in the V_{oc} versus electron density plots, on the other hand, does not support this hypothesis. A possible explanation for this discrepancy is the different electron density range over which these measurements typically operate. Because of charge extraction, the electron density at short circuit can be an order of magnitude smaller than that at open circuit. Charge extraction measurements extended to much lower electron densities could resolve this issue. Furthermore, a study of the effects of light exposure as a function of electrolyte composition, cation size and mobility, and solvent viscosity is currently underway. These results indicate a direct correlation between electron lifetime increase and diffusion coefficient decrease, suggesting the possible involvement of photogenerated electron traps. Further measurements involving the systematic variation of the electrolyte composition are ongoing and will be reported elsewhere.

Conclusions

A significant improvement in all photovoltaic parameters of porphyrin-sensitized DSSCs was observed after 1 h of light exposure. The increased short-circuit current is attributed to improved charge injection, demonstrated by thin-film APCE measurements. No change in the dye regeneration kinetics, studied by transient absorption spectroscopy, was observed. Improved electron lifetimes and decreased electron diffusion coefficients were measured using transient photovoltage/photocurrent measurements, which might suggest the photogeneration of subgap electron trap states during white light illumination. No change in the V_{oc} versus electron density plot was recorded, suggesting that the improvement is not due to a shift in the CB potential as proposed previously. Electrochemical impedance spectroscopy performed before and after light exposure revealed changes at both the TiO_2−dye-electrolyte and electrolyte−Pt counter electrode interfaces. A reduction in charge-transfer impedance for I_3^- recycling is proposed to explain the improvement in the electrical fill factor of the solar cells. ATR-FTIR and X-ray reflectometry measurements indicated no major change of the dye binding mode or dye layer thickness within the first hour of light exposure, which suggests that the effect is not related to morphology changes of the dye layer.

Acknowledgment. M.J.G., A.J.M., P.W., D.L.O., and G.G.W. acknowledge the support of the Australian Research Council through the ARC Center of Excellence, Federation Fellowship, Discovery, and LIEF schemes. K.W., A.J.M., G.T., and D.L.O. acknowledge the support of CRC for Polymers. M.J.G. acknowledges the support of a Prime Minister's Australia Asia Endeavour Award from the Australian Department of Education, Employment and Workplace Relations. The authors thank the Australian Synchrotron for financial support of the FTIR work undertaken on the infrared microspectroscopy beamline, with special thanks to Dr. Mark Tobin and Dr. Ljiljana Puskar for their additional technical support. The authors also thank Professor Shogo Mori for fruitful discussions.

Supporting Information Available: Synthesis of (*E*) 3-(4-dimethylaminophenyl)propenylidenemalonic acid, FTIR spectrum of GD2 porphyrin dye bound to TiO_2 and its free di(tetra-n-butylammonium salt) and geometry-optimized molecular structure of GD2 porphyrin dye on a TiO_2 cluster showing dye size and proposed binding angle. This material is available free of charge via the Internet at http://pubs.acs.org.

References and Notes

(1) (a) O'Regan, B.; Grätzel, M. *Nature* **1991**, *353*, 737. (b) Nazeeruddin, M. K.; Kay, A.; Rodicio, I.; Humphry-Baker, R.; Müller, E.; Liska, P.; Vlachopoulos, N.; Grätzel, M. *J. Am. Chem. Soc.* **1993**, *115*, 6382. (c) Grätzel, M. *Acc. Chem. Res.* **2009**, *42*, 1788.

(2) (a) Grätzel, M. *Nature* **2001**, *414*, 338. (b) Katoh, R.; Furube, A.; Barzykin, A. V.; Arakawa, H.; Tachiya, M. *Coord. Chem. Rev.* **2004**, *248*, 1195. (c) Durrant, J. R.; Haque, S. A.; Palomares, E. *Coord. Chem. Rev.* **2004**, *248*, 1247. (d) Koops, S. E.; O'Regan, B. C.; Barnes, P. R. F.; Durrant, J. R. *J. Am. Chem. Soc.* **2009**, *131*, 4808.

(3) (a) He, J. J.; Lindstrom, H.; Hagfeldt, A.; Lindquist, S. E. *J. Phys. Chem. B* **1999**, *103*, 8940. (b) Mori, S.; Fukuda, S.; Sumikura, S.; Takeda, Y.; Tamaki, Y.; Suzuki, E.; Abe, T. *J. Phys. Chem. C* **2008**, *112*, 16134. (c) Nattestad, A.; Mozer, A. J.; Fischer, M. K. R.; Cheng, Y.-B.; Mishra, A.; Bäuerle, P.; Bach, U. *Nat. Mater.* **2010**, *9*, 31.

(4) (a) Kalyanasundaram, K.; Vlachopoulos, N.; Krishnan, V.; Monnier, A.; Graetzel, M. *J. Phys. Chem.* **1987**, *91*, 2342. (b) Kay, A.; Graetzel, M. *J. Phys. Chem.* **1993**, *97*, 6272. (c) Boschloo, G. K.; Goossens, A. *J. Phys. Chem.* **1996**, *100*, 19489.

(5) (a) Campbell, W. M.; Burrell, A. K.; Officer, D. L.; Jolley, K. W. *Coord. Chem. Rev.* **2004**, *248*, 1363. (b) Wang, Q.; Campbell, W. M.; Bonfantani, E. E.; Jolley, K. W.; Officer, D. L.; Walsh, P. J.; Gordon, K.; Humphry-Baker, R.; Nazeeruddin Mohammad, K.; Gratzel, M. *J. Phys. Chem. B* **2005**, *109*, 15397. (c) Campbell, W. M.; Jolley, K. W.; Wagner, P.; Wagner, K.; Walsh, P. J.; Gordon, K. C.; Schmidt-Mende, L.; Nazeeruddin, M. K.; Wang, Q.; Graetzel, M.; Officer, D. L. *J. Phys. Chem. C* **2007**, *111*, 11760. (d) Imahori, H.; Umeyama, T.; Ito, S. *Acc. Chem. Res.* **2009**, *42*, 1809. (e) Lee, C.-W.; Lu, H.-P.; Lan, C.-M.; Huang, Y.-L.; Liang, Y.-R.; Yen, W.-N.; Liu, Y.-C.; Lin, Y.-S.; Diau, E. W.-G.; Yeh, C.-Y. *Chem.—Eur. J.* **2009**, *15*, 1403. (f) Chen, C.-C.; Chung, H.-W.; Chen, C.-H.; Lu, H.-P.; Lan, C.-M.; Chen, S.-F.; Luo, L.; Hung, C.-S.; Diau, E. W.-G. *J. Phys. Chem. C* **2008**, *112*, 19151. (g) Forneli, A.; Planells, M.; Sarmentero, M. A.; Martinez-Ferrero, E.; O'Regan, B. C.; Ballester, P.; Palomares, E. *J. Mater. Chem.* **2008**, *18*, 1652.

(6) Dos Santos, T.; Morandeira, A.; Koops, S.; Mozer, A. J.; Tsekouras, G.; Dong, Y.; Wagner, P.; Wallace, G.; Earles, J. C.; Gordon, K. C.; Officer, D.; Durrant, J. R. *J. Phys. Chem. C* **2010**, *114*, 3276.

(7) (a) Koehorst, R. B. M.; Boschloo, G. K.; Savenije, T. J.; Goossens, A.; Schaafsma, T. J. *J. Phys. Chem. B* **2000**, *104*, 2371. (b) Martinson, A. B. F.; Hamann, T. W.; Pellin, M. J.; Hupp, J. T. *Chem.—Eur. J.* **2008**, *14*, 4458. (c) Mozer, A. J.; Griffith, M. J.; Tsekouras, G.; Wagner, P.; Wallace, G. G.; Mori, S.; Sunahara, K.; Miyashita, M.; Earles, J. C.; Gordon, K. C.; Du, L.; Katoh, R.; Furube, A.; Officer, D. L. *J. Am. Chem. Soc.* **2009**, *131*, 15621. (d) Mai, C.-L.; Huang, W.-K.; Lu, H.-P.; Lee, C.-W.; Chiu, C.-L.; Liang, Y.-R.; Diau, E. W.-G.; Yeh, C.-Y. *Chem. Commun.* **2010**, *46*, 809. (e) Park, J. K.; Chen, J.; Lee, H. R.; Park, S. W.; Shinokubo, H.; Osuka, A.; Kim, D. *J. Phys. Chem. C* **2009**, *113*, 21956.

(8) (a) Lo, C.-F.; Luo, L.; Diau, E. W.-G.; Chang, I.-J.; Lin, C.-Y. *Chem. Commun.* **2006**, 1430. (b) Galoppini, E. *Coord. Chem. Rev.* **2004**, *248*, 1283. (c) Lin, C.-Y.; Lo, C.-F.; Luo, L.; Lu, H.-P.; Hung, C.-S.; Diau, E. W.-G. *J. Phys. Chem. C* **2009**, *113*, 755.

(9) (a) Tachibana, Y.; Haque, S. A.; Mercer, I. P.; Durrant, J. R.; Klug, D. R. *J. Phys. Chem. B* **2000**, *104*, 1198. (b) Clifford, J. N.; Yahioglu, G.; Milgrom, L. R.; Durrant, J. R. *Chem. Commun.* **2002**, 1260. (c) Clifford, J. N.; Palomares, E.; Nazeeruddin, M. K.; Graetzel, M.; Nelson, J.; Li, X.; Long, N. J.; Durrant, J. R. *J. Am. Chem. Soc.* **2004**, *126*, 5225. (d) Ma, T.; Inoue, K.; Noma, H.; Yao, K.; Abe, E. *J. Photochem. Photobiol. A: Chemistry* **2002**, *152*, 207. (e) Watson, D. F.; Marton, A.; Stux, A. M.; Meyer, G. J. *J. Phys. Chem. B* **2004**, *108*, 11680. (f) Hsieh, C.-P.; Lu, H.-P.; Chiu, C.-L.; Lee, C.-W.; Chuang, S.-H.; Mai, C.-L.; Yen, W.-N.; Hsu, S.-J.; Diau, E. W.-G.; Yeh, C.-Y. *J. Mater. Chem.* **2010**, *20*, 1127. (g) Rochford, J.; Chu, D.; Hagfeldt, A.; Galoppini, E. *J. Am. Chem. Soc.* **2007**, *129*, 4655. (h) Rochford, J.; Galoppini, E. *Langmuir* **2008**, *24*, 5366. (i) Rio, Y.; Vazquez, P.; Palomares, E. *J. Porphyrins Phthalocyanines* **2009**, *13*, 645. (j) Stromberg, J. R.; Marton, A.; Kee, H. L.; Kirmaier, C.; Diers, J. R.; Muthiah, C.; Taniguchi, M.; Lindsey, J. S.; Bocian, D. F.; Meyer, G. J.; Holten, D. *J. Phys. Chem. C* **2007**, *111*, 15464.

(10) (a) Imahori, H.; Hayashi, S.; Umeyama, T.; Eu, S.; Oguro, A.; Kang, S.; Matano, Y.; Shishido, T.; Ngamsinlapasathian, S.; Yoshikawa, S. *Langmuir* **2006**, *22*, 11405. (b) Tanaka, M.; Hayashi, S.; Eu, S.; Umeyama, T.; Matano, Y.; Imahori, H. *Chem. Commun.* **2007**, 2069. (c) Eu, S.; Hayashi, S.; Umeyama, T.; Matano, Y.; Araki, Y.; Imahori, H. *J. Phys. Chem. C* **2008**, *112*, 4396. (d) Imahori, H.; Hayashi, S.; Hayashi, H.; Oguro, A.; Eu, S.; Umeyama, T.; Matano, Y. *J. Phys. Chem. C* **2009**, *113*, 18406. (e) Imahori, H.; Matsubara, Y.; Iijima, H.; Umeyama, T.; Matano, Y.; Ito, S.; Niemi, M.; Tkachenko, N. V.; Lemmetyinen, H. *J. Phys. Chem. C* **2010**, *114*, 10656. (f) Kira, A.; Matsubara, Y.; Iijima, H.; Umeyama, T.; Matano, Y.; Ito, S.; Niemi, M.; Tkachenko, N. V.; Lemmetyinen, H.; Imahori, H. *J. Phys. Chem. C* **2010**, *114*, 11293.

(11) Mozer, A. J.; Wagner, P.; Officer, D. L.; Wallace, G. G.; Campbell, W. M.; Miyashita, M.; Sunahara, K.; Mori, S. *Chem. Commun.* **2008**, 4741.

(12) Allegrucci, A.; Lewcenko, N. A.; Mozer, A. J.; Dennany, L.; Wagner, P.; Officer, D. L.; Sunahara, K.; Mori, S.; Spiccia, L. *Energy Environ. Sci.* **2009**, *2*, 1069.

(13) Wang, Q.; Zhang, Z.; Zakeeruddin, S. M.; Grätzel, M. *J. Phys. Chem. C* **2008**, *112*, 7084.

(14) Ferrere, S.; Gregg, B. A. *J. Phys. Chem. B* **2001**, *105*, 7602.

(15) Gregg, B. A.; Chen, S.-G.; Ferrere, S. *J. Phys. Chem. B* **2003**, *107*, 3019.

(16) Sauvage, F.; Fischer, M. K. R.; Mishra, A.; Shaik, M.; Zakeeruddin, S. M.; Nazeeruddin, M. K.; Bäuerle, P.; Grätzel, M. *ChemSusChem* **2009**, *2*, 761.

(17) Ito, S.; Nazeeruddin, M. K.; Liska, P.; Comte, P.; Charvet, R.; Pechy, P.; Jirousek, M.; Kay, A.; Zakeeruddin, S. M.; Grätzel, M. *Prog. Photovoltaics: Res. Appl.* **2006**, *14*, 589.

(18) Kubo, W.; Sakamoto, A.; Kitamura, T.; Wada, Y.; Yanagida, S. *J. Photochem. Photobiol. A: Chem.* **2004**, *164*, 33.

(19) Nakade, S.; Kanzaki, T.; Wada, Y.; Yanagida, S. *Langmuir* **2005**, *21*, 10803.

(20) Peter, L. M.; Duffy, N. W.; Wang, R. L.; Wijayantha, K. G. U. J. *Electroanal. Chem.* **2002**, *524*, 127.

(21) Triani, G.; Evans, P. J.; Mitchell, D. R. G.; Attard, A. J.; Finnie, K. S.; James, M.; Hanley, T.; Latella, B.; Prince, K. E.; Bartlett, J. In *Advances in Thin-Film Coatings for Optical Applications II (Proceedings of SPIE)*; Fulton, M. L., Kruschwitz, J. D., Eds.; SPIE: Bellingham, WA, 2005; Vol. 5870, p 587009.

(22) Nelson, A. *J. Appl. Crystallogr.* **2006**, *39*, 273.

(23) (a) Sommeling, P. M.; Späth, M.; Smit, H. J. P.; Bakker, N. J.; Kroon, J. M. *J. Photochem. Photobiol. A: Chem.* **2004**, *164*, 137. (b) Likodimos, V.; Stergiopoulos, T.; Falaras, P.; Harikisun, R.; Desilvestro, J.; Tulloch, G. *J. Phys. Chem. C* **2009**, *113*, 9412.

(24) (a) Arakawa, H.; Yamaguchi, T.; Okada, K.; Matsui, H.; Kitamura, T.; Tanabe, N. *Fujikura Tech. Rev.* **2009**, 55. (b) Andrade, L.; Zakeeruddin, S. M.; Nazeeruddin, M. K.; Ribeiro, H. A.; Mendes, A.; Grätzel, M. *Int. J. Chem. Eng.* **2009**, article 563420;, http://dx.doi.org/10.1155/2009/563420.

(25) Zakeeruddin, S. M.; Nazeeruddin, Md. K.; Humphry-Baker, R.; Péchy, P.; Quagliotto, P.; C. Barolo, C.; G. Viscardi, G.; M. Grätzel, M. *Langmuir* **2002**, *18*, 952.

(26) (a) Kopidakis, N.; Benkstein, K. D.; van de Lagemaat, J.; Frank, A. J. *J. Phys. Chem. B* **2003**, *107*, 11307. (b) Nelson, J. *Phys. Rev. B* **1999**, *59*, 15374.

(27) Bisquert, J. *J. Phys. Chem. B* **2002**, *106*, 325.

(28) Hoshikawa, T. T.; M. Yamada, M.; R. Kikuchi, R.; Eguchi, K. *J. Electrochem. Soc.* **2005**, *152*, E68.

(29) Wang, Q.; Ito, S.; Grätzel, M.; Fabregat-Santiago, F.; Mora-Sero, I.; Bisquert, J.; Bessho, T.; Imai, H. *J. Phys. Chem. B* **2006**, *110*, 25210.

(30) Wang, Q.; Moser, J.-E.; Grätzel, M. *J. Phys. Chem. B* **2005**, *109*, 14945.

(31) Tsekouras, G.; Mozer, A. J.; Wallace, G. G. *J. Electrochem. Soc.* **2008**, *155*, K124–K128.

(32) Srinivas, K.; Yesudas, K.; Bhanuprakash, K.; Rao, V. J.; Giribabu, L. *J. Phys. Chem. C* **2009**, *113*, 20117.

(33) Deacon, G. B.; Phillips, R. J. *Coord. Chem. Rev.* **1980**, *33*, 227.

(34) Nazeeruddin, M. K.; Humphry-Baker, R.; Officer, D. L.; Campbell, W. M.; Burrell, A. K.; Grätzel, M. *Langmuir* **2004**, *20*, 6514.

(35) Wiberg, J.; Marinado, T.; Hagberg, D. P.; Sun, L.; Hagfeldt, A.; Albinsson, B. *J. Phys. Chem. B* **2010**, *114*, 14358.

JP107615H